Order online now!

www.rockland.com
tech@rockland.com
+1 484.791.3823

Datasheet for MB-008

10X PBS pH 7.2

Overview

Description:	10X PBS pH 7.2 (0.2 M Potassium Phosphate 1.5 M Sodium Chloride) - MB-008
Item No.:	MB-008
Size:	1 L
Applications:	ELISA, FC, IF, Other

Product Details

Background:	Phosphate buffered saline is suitable for multiple applications including biological diluent buffer for antibodies or other biologics. Also may be used as a wash buffer for immunological assays including western blot, immunohistochemistry, immunofluorescence microscopy, and ELISA. Other applications may require detergents or other additional components.
Synonyms:	Phosphate buffered saline, Phosphate buffered solution, PBS, 10X PBS

Target Details

Purity/Specificity:	10X PBS buffer was aseptically filtered through a Millipore 0.22 micron filter into clean, pre-sterilized containers. The product was tested on trypticase soy agar for 24 hours, 48 hours and 72 hours and was found to be negative for bacteria.
Relevant Links:	• MB-008 SDS

Application Details

Suggested Applications:	ELISA, FC, IF, Other (Based on references)
Application Note:	This product is a concentrated stock solution and should be diluted appropriately with distilled, deionized water or equivalent to its final working concentration. 10X Phosphate Buffered Saline (PBS) consists of 0.2 M Potassium Phosphate, 1.5 M Sodium Chloride, pH 7.2 prepared in highly polished pharmaceutical grade water (WFI).
Assay Dilutions:	All assays should be optimized by the user. Recommended dilutions (if any) may be listed below.
ELISA:	User Optimized

WB:	User Optimized

Formulation

Physical State:	Liquid
Concentration:	10X
Buffer:	See application note.
Preservative:	None
Stabilizer:	None

Shipping & Handling

Shipping Condition:	Ambient
Storage Condition:	Store container at room temperature (18° to 26° C) prior to opening. If desired, the solution may be stored at 4° C or less. Some salts may precipitate out of solution at lower temperature. Allow buffer to equilibrate to room temperature (18° to 26° C) to restore solubility of some salts.
Expiration:	Expiration date is six (6) months from date of receipt.

Images

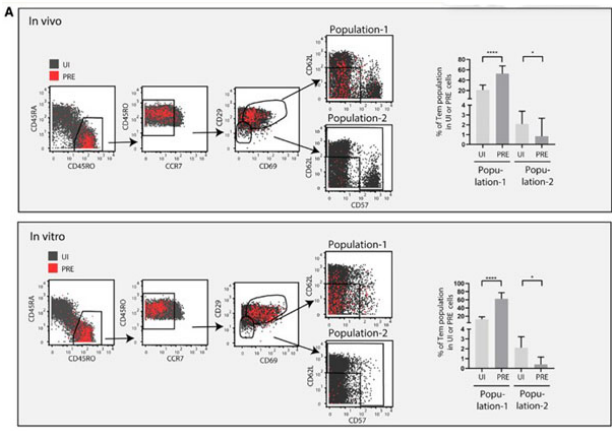

Flow Cytometry

A subset of Tem-like cells sorted based on surface markers defining clusters 12 and 13 are highly susceptible to HIV infection. (A) Shown are the CyTOF datasets, with UI CD4+ T cells shown in gray and the HIV-susceptible PRE cells shown in red. Cells were pre-gated on live, singlet CD3+CD19−CD8−CD4+ T cells. A sequential gating strategy was then implemented using surface markers characteristic of HIV-susceptible cells as defined by clusters 12 and 13. This strategy was used to characterize a final population of "population-1" cells (CD3+CD4+CD45RO +CD45RA−CCR7low/medCD29med/highCD69med/high CD62 LlowCD57low/med), which were more abundant among PRE cells than among UI cells. For comparison, we characterized a "population-2" (CD3+CD4+CD45RO +CD45RA−CCR7low/medCD29lowCD69low and not CD62LlowCD57low/med) predicted to be much less susceptible to infection because it comprised a significantly lower proportion of PRE cells. The gating strategies are shown on the left, whereas the graphs on the right depict the frequencies of the population-1 and population-2 subsets within the UI and PRE cell populations. Note that the over-representation of population-1 cells among PRE cells suggest their preferential susceptibility to infection, whereas the under-representation of population-2 cells among PRE cells suggest their relative resistance to infection. *p < 0.05, ****p < 0.0001 as determined by a Student's paired t test. Error bars correspond to the standard deviation.
Figure 7. PMID: 33910003.

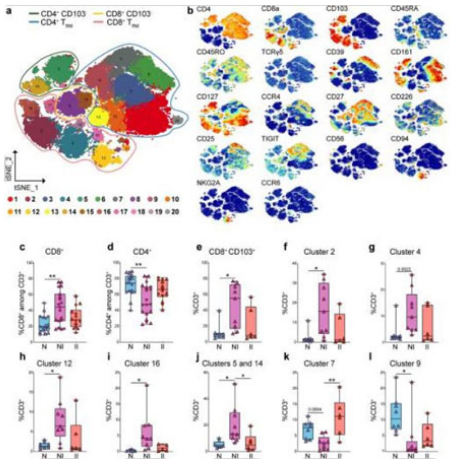

Flow Cytometry
Quantification of CD8 and CD4 T cell clusters by CyTOF analysis in LP of control and CD patients. a Schematic t-SNE of CD4+ and CD8+ T cells from LP of all donors concatenated together (n = 18) controls (N), n = 8; CD, non-inflamed site (NI), n = 9; CD, inflamed site (II), n = 6. Total of 23 samples. b t-SNE of the indicated markers in CD4+ and CD8+ T cells. c, d Quantification of total CD8+ (c), total CD4+ (d) in LP of controls and CD patients by CyTOF (triangles = fresh samples) and FACS (circles = frozen samples). c, d Control (N), n = 17 (8 fresh, 9 frozen); CD, non-inflamed site (NI) n = 19 (9 fresh, 10 frozen); CD, inflamed site (II), n = 14 (6 fresh, 8 frozen). e–i Quantification of total CD8+ TRM (e) and CD8+ clusters 2 (f), 4 (g), 12 (h), and 16 (i) in LP of controls and CD patients by CyTOF. j–l Quantification of the CD4+ clusters 5 and 14 (j), 7 (k), and 9 (l) in LP of controls and CD patients by CyTOF. e–l Controls (N), n = 8; CD, non-inflamed site (NI), n = 9; CD, inflamed site (II), n = 6. Circles and triangles on the boxplots show data collected for each individual donor. Data were median and interquartile range. Significance was calculated using an ordinary, one-way ANOVA, multiple comparisons test with Prism v8 software. c **P = 0.0014; d **P = 0.028; e *P = 0.0139; f *P = 0.0178; h *P = 0.0178; i *P = 0.0219; j N vs. NI *P = 0.0156, NI vs. II *P = 0.0465; k **P = 0.0014; l **P = 0.0283. TRM tissue-resident memory T cell. Fig. 6. PMID: 33771991.



Bottle
10X PBS pH 7.2 (0.2 M Potassium Phosphate 1.5 M Sodium Chloride)

References

- Donovan MG et al. Systematic multi-omic deconvolution of the clinical heterogeneity of Down syndrome. *Nat Commun.* (2026)
- Ma T et al. Persistent cytolytic CD8+ T cells recognize SARS-CoV-2 and herpesvirus epitopes in long COVID. *Cell Rep Med.* (2026)
- de Los Rios Kobara I et al. Viral load-driven systemic immune exhaustion is an enabler of antibody breadth in HIV infection. *BioRxiv [Preprint].* (2026)
- Ma T et al. Multiomic analysis of ART-interruption cohorts identifies cell-extrinsic and -intrinsic mechanisms driving lymphocyte-mediated control of HIV rebound. *Immunity.* (2026)
- Dunn LN et al. Altered hepatic metabolism in Down syndrome. *Cell Rep.* (2026)
- Søndergaard JN et al. Assessing Human Treg Suppression at Single-Cell Resolution Using Mass Cytometry. *Bio Protoc.* (2025)
- George AF et al. Anatomical, subset, and HIV-dependent expression of viral sensors and restriction factors. *Cell Rep.* (2025)
- Pi R et al. NKp30 and NKG2D contribute to natural killer cell-mediated recognition of HIV-infected cells. *iScience.* (2025)
- Liang Y et al. Persistent lymphopenia after kidney transplantation: increased mortality and decreased homeostatic mechanisms. *Front Immunol.* (2025)
- Søndergaard JN et al. Single cell suppression profiling of human regulatory T cells. *Nat Commun.* (2025)
- Dudziak D et al. Guidelines for preparation and flow cytometry analysis of human nonlymphoid tissue DC. *Eur J Immunol.* (2025)
- Kowli S et al. Characterization of immune phenotypes in peripheral blood of adult renal transplant recipients using mass cytometry (CyTOF). *Immunohorizons.* (2025)
- Patel SP et al. Phase II basket trial of Dual Anti-CTLA-4 and anti-PD-1 blockade in Rare Tumors (DART) SWOG S1609: pancreatic neuroendocrine neoplasm (PNEN) cohort. *J Immunolther Cancer.* (2025)
- Yin K et al. Pregnancy and lactation induce distinct immune responses to COVID-19 booster vaccination and SARS-CoV-2 breakthrough infection. *JCI Insight.* (2025)
- Eduthan NP et al. An integrated multi-omic natural history study of human development, sexual dimorphism, and the effects of trisomy 21. *Nat Commun.* (2025)
- Gupta S et al. Cellular immune changes during severe antisense oligonucleotide-associated thrombocytopenia in a nonhuman primate model. *J Immunol.* (2025)
- Tan Z et al. Immune development differs between preterm newborns fed mothers' own milk and donor milk. *iScience.* (2025)
- Zhang R et al. Biofilm Formation in Clinical Isolates of Fusarium. *J Fungi (Basel).* (2024)
- Cao S et al. Single-Cell and Spatial Multi-omics Reveal Interferon Signaling in the Pathogenesis of Perianal Fistulizing Crohn's Disease. *BioRxiv [Preprint].* (2024)
- Donovan MG et al. Multimodal analysis of dysregulated heme metabolism, hypoxic signaling, and stress erythropoiesis in Down syndrome. *Cell Rep.* (2024)

- Seo Y et al. Barcoding of viable peripheral blood mononuclear cells with selenium and tellurium isotopes for mass cytometry experiments. *Cytometry A.* (2024)
- Mohamad SF et al. Utilizing CyTOF to Examine Hematopoietic Stem and Progenitor Phenotype. *Methods Mol Biol.* (2023)
- Sperber HS et al. The hypoxia-regulated ectonucleotidase CD73 is a host determinant of HIV latency. *Cell Rep.* (2023)
- Sanz M et al. Aminobisphosphonates reactivate the latent reservoir in people living with HIV-1. *Front Immunol.* (2023)
- Galbraith MD et al. Multidimensional definition of the interferonopathy of Down syndrome and its response to JAK inhibition. *Sci Adv.* (2023)
- Gihring A et al. Influence of bariatric surgery on the peripheral blood immune system of female patients with morbid obesity revealed by high-dimensional mass cytometry. *Front Immunol.* (2023)
- Lança T et al. IRF8 deficiency induces the transcriptional, functional, and epigenetic reprogramming of cDC1 into the cDC2 lineage. *Immunity.* (2022)
- Agosto-Burgos C et al. The frequency of Treg subsets distinguishes disease activity in ANCA vasculitis. *Clin Transl Immunology.* (2022)
- Su C et al. 3D chromatin maps of the human pancreas reveal lineage-specific regulatory architecture of T2D risk. *Cell Metab.* (2022)
- Henrick BM et al. Bifidobacteria-mediated immune system imprinting early in life. *Cell.* (2021)
- Xie G et al. Characterization of HIV-induced remodeling reveals differences in infection susceptibility of memory CD4+ T cell subsets in vivo. *Cell Rep.* (2021)
- Sahaf, B et al. Immune Profiling Mass Cytometry Assay Harmonization: Multicenter Experience from CIMAC-CIDC. *Clinical Cancer Research : An Official Journal of the American Association for Cancer Research* (2021)
- Jaeger N et al. Single-cell analyses of Crohn's disease tissues reveal intestinal intraepithelial T cells heterogeneity and altered subset distributions. *Nat Commun.* (2021)
- Neidleman J et al. Distinctive features of SARS-CoV-2-specific T cells predict recovery from severe COVID-19. *medRxiv.* (2021)
- Vasudevan S et al. Lower PDL1, PDL2, and AXL Expression on Lung Myeloid Cells Suggests Inflammatory Bias in Smoking and Chronic Obstructive Pulmonary Disease. *Am J Respir Cell Mol Biol.* (2020)
- Lakshmikanth T et al. Human immune system variation during 1 year. *Cell Rep.* (2020)
- Sahaf B et al. High-parameter immune profiling with CyTOF. *Methods Mol Biol.* (2020)
- Colomb F et al. Sialyl-LewisX Glycoantigen Is Enriched on Cells with Persistent HIV Transcription during Therapy. *Cell Rep.* (2020)
- Vendrame E et al. Profiling of the Human Natural Killer Cell Receptor-Ligand Repertoire. *J Vis Exp.* (2020)
- Fenton TM et al. Immune profiling of human gut-associated lymphoid tissue identifies a role for isolated lymphoid follicles in priming of region-specific immunity. *Immunity.* (2020)
- Rodriguez L et al. Systems-Level Immunomonitoring from Acute to Recovery Phase of Severe COVID-19 *Cell Rep Med.* (2020)

- Neidleman J et al. SARS-CoV-2-specific T cells exhibit phenotypic features of helper function, lack of terminal differentiation, and high proliferation potential. *Cell Rep Med.* (2020)
- Waugh KA et al. Mass cytometry reveals global immune remodeling with multi-lineage hypersensitivity to type I interferon in Down syndrome. *Cell Rep.* (2019)
- Cella M et al. Subsets of ILC3-ILC1-like cells generate a diversity spectrum of innate lymphoid cells in human mucosal tissues. *Nat Immunol.* (2019)
- Collins PL et al. Gene regulatory programs conferring phenotypic identities to human NK cells. *Cell.* (2019)
- Fernandez J et al. Isolation and Staining of Mouse Skin Keratinocytes for Cell Cycle Specific Analysis of Cellular Protein Expression by Mass Cytometry. *J Vis Exp.* (2019)
- Cella, M et al. Subsets of ILC3-ILC1-like cells generate a diversity spectrum of innate lymphoid cells in human mucosal tissues. *Nature Immunology* (2019)
- Leipold MD et al. Comparison of CyTOF assays across sites: Results of a six-center pilot study. *J Immunol Methods.* (2018)
- Olin A et al. Stereotypic immune system development in newborn children. *Cell.* (2018)
- Subrahmanyam PB et al. Cytof measurement of immunocompetence across major immune cell types. *Curr Protoc Cytom.* (2017)
- Leipold MD et al. Phenotyping of live human PBMC using CyTOFTM mass cytometry. *Bio Protoc.* (2015)
- Lin D et al. Intracellular cytokine staining on PBMCs Using CyTOF™ mass cytometry. *Bio Protoc.* (2015)
- Fernandez R et al. Cytokine-stimulated phosphoflow of PBMC using CyTOF mass cytometry. *Bio Protoc.* (2015)
- Fernandez, R et al. Cytokine-Stimulated Phosphoflow of Whole Blood Using CyTOF Mass Cytometry. *Bio-Protocol* (2015)
- Gupta S et al. Intracellular Cytokine Staining (ICS) on Human Lymphocytes or Peripheral Blood Mononuclear Cells (PBMCs). *Bio Protoc.* (2015)
- JENNIFER BERGER GENE EXPRESSION PATTERNS OF GAMMAHERPESVIRUSES. *Olaf College* (2012)

Disclaimer

This product is for research use only and is not intended for therapeutic or diagnostic applications. Please contact a technical service representative for more information. All products of animal origin manufactured by Rockland Immunochemicals are derived from starting materials of North American origin. Collection was performed in United States Department of Agriculture (USDA) inspected facilities and all materials have been inspected and certified to be free of disease and suitable for exportation. All properties listed are typical characteristics and are not specifications. All suggestions and data are offered in good faith but without guarantee as conditions and methods of use of our products are beyond our control. All claims must be made within 30 days following the date of delivery. The prospective user must determine the suitability of our materials before adopting them on a commercial scale. Suggested uses of our products are not recommendations to use our products in violation of any patent or as a license under any patent of Rockland Immunochemicals, Inc. If you require a commercial license to use this material and do not have one, then return this material, unopened to: Rockland Inc., P.O. BOX 5199, Limerick, Pennsylvania, USA.